

# 9-ING-41, a small-molecule glycogen synthase kinase-3 inhibitor, is active in neuroblastoma

Andrey V. Ugolkov<sup>a,d</sup>, Gennadiy I. Bondarenko<sup>d</sup>, Oleksii Dubrovskiy<sup>d</sup>, Ana P. Berbegall<sup>e,f</sup>, Samuel Navarro<sup>e,f</sup>, Rosa Noguera<sup>e,f</sup>, Thomas V. O'Halloran<sup>c,d</sup>, Mary J. Hendrix<sup>c</sup>, Francis J. Giles<sup>a,c</sup> and Andrew P. Mazar<sup>b,c,d</sup>

Advanced stage neuroblastoma is a very aggressive pediatric cancer with limited treatment options and a high mortality rate. Glycogen synthase kinase-3 $\beta$  (GSK-3 $\beta$ ) is a potential therapeutic target in neuroblastoma. Using immunohistochemical staining, we observed positive GSK-3 $\beta$  expression in 67% of human neuroblastomas (34 of 51 cases). Chemically distinct GSK-3 inhibitors (AR-A014418, TDZD-8, and 9-ING-41) suppressed the growth of neuroblastoma cells, whereas 9-ING-41, a clinically relevant small-molecule GSK-3 $\beta$  inhibitor with broad-spectrum preclinical antitumor activity, being the most potent. Inhibition of GSK-3 resulted in a decreased expression of the antiapoptotic molecule XIAP and an increase in neuroblastoma cell apoptosis. Mouse xenograft studies showed that the combination of clinically relevant doses of CPT-11 and 9-ING-41 led to greater antitumor effect than was observed with either agent alone. These data support

the inclusion of patients with advanced neuroblastoma in clinical studies of 9-ING-41, especially in combination with CPT-11. *Anti-Cancer Drugs* 00:000–000 Copyright © 2018 Wolters Kluwer Health, Inc. All rights reserved.

*Anti-Cancer Drugs* 2018, 00:000–000

**Keywords:** 9-ING-41, chemoresistance, CPT-11, glycogen synthase kinase-3, glycogen synthase kinase-3 $\beta$ , irinotecan, neuroblastoma

<sup>a</sup>Department of Medicine, Developmental Therapeutic Program, Division of Hematology/Oncology, <sup>b</sup>Department of Pharmacology, Feinberg School of Medicine, Northwestern University, <sup>c</sup>Robert H. Lurie Comprehensive Cancer Center of Northwestern University, Chicago, <sup>d</sup>Chemistry of Life Processes Institute, Northwestern University, Evanston, Illinois, <sup>e</sup>Department of Pathology, Medical School, University of Valencia-INCLIVA, Valencia and <sup>f</sup>Cancer CIBER (CIBERONC), Madrid, Spain

Correspondence to Andrew P. Mazar, PhD, Monopar Therapeutics, Inc. 5 Revere Drive, Suite 200, Northbrook, IL 60062, USA  
Tel: +1 847 388 0349 x403; e-mail: mazar@monoparx.com

Received 23 March 2018 Revised form accepted 1 May 2018

## Introduction

Neuroblastoma is one of the commonest and most lethal pediatric solid tumors and is believed to reflect aberrant differentiation of the developing sympathoadrenergic lineage of the neural crest [1,2]. Neuroblastoma exhibits marked intratumoral and intertumoral heterogeneity, with high-risk tumors characterized by poor differentiation and chemoresistance [1,2]. The current 5-year survival rate for patients with high-risk neuroblastoma is less than 50% despite aggressive and multimodal treatment [1]. Thus, this malignancy represents a significant unmet medical need, and the identification of new therapeutic agents is urgently needed.

Glycogen synthase kinase-3 (GSK-3), a serine/threonine kinase, is a master regulator of neural progenitor homeostasis, integrating multiple proliferation, and differentiation signals, and thus has been focused on as a potential target in neuroblastoma [3]. Previous studies showed that GSK-3 $\beta$  is a positive regulator of nuclear factor- $\kappa$ B (NF- $\kappa$ B)-mediated survival and chemoresistance of cancer cells [4–10]. Inhibition of the NF- $\kappa$ B signaling pathway has been shown to induce apoptosis in neuroblastoma cells [11,12]. An increase of NF- $\kappa$ B transcriptional activity has been reported in neuroblastoma cells treated with doxorubicin or etoposide [13]. Previous reports have

shown that tool compound, nonclinically applicable, GSK-3 inhibitors reduced the cell viability, by apoptosis induction, in a range of neuroblastoma cell lines, including those derived from clinically high-risk MYCN-amplified metastatic tumors, while not affecting the viability of differentiated neurons [14–17].

In the present study, we evaluated the antitumor effects of a clinical stage drug, 9-ING-41, a small-molecule inhibitor of GSK-3, in neuroblastoma cell lines and xenograft tumors. Previous studies have showed drug-like properties of 9-ING-41, including good tolerability and antitumor activity in rodents [18–20]. Recent studies have shown that 9-ING-41 significantly enhanced the efficacy of chemotherapeutic drugs in glioblastoma and breast patient-derived xenograft (PDX) tumor models [21,22]. Here, we demonstrate that GSK-3 $\beta$  expression is highly prevalent in human neuroblastomas and that the GSK-3 inhibitor 9-ING-41 is a potential therapeutic agent for the treatment of human neuroblastoma.

## Materials and methods

### Cell culture and reagents

Neuroblastoma cell lines SK-N-DZ and SK-N-BE(2) were obtained from American Type Culture Collection

(Manassas, Virginia, USA). The GSK-3 inhibitor 9-ING-41 was provided by Actuate Therapeutics Inc. (Forth Worth, Texas, USA). SK-N-DZ cell line was established from metastatic poorly differentiated neuroblastoma with *MYCN* amplification, 11q deletion and *TP53* mutation. SK-N-BE(2) cell line was established from a metastatic neuroblastoma with *MYCN* amplification and *TP53* mutation. All other chemicals were obtained from Sigma (St. Louis, Missouri, USA).

### Measurement of cell viability

Relative number of viable cancer cells was determined by measuring the optical density using CellTiter 96 Aqueous One Solution Cell Proliferation Assay kit [3-(4,5-dimethylthiazol-2-yl)-5-(3-carboxymethoxyphenyl)-2-(4-sulfophenyl)-2H-tetrazolium, inner salt] according to the manufacturer's instructions (Promega, Madison, Wisconsin, USA). A  $GI_{50}$  value for each compound was calculated with a nonlinear regression model of standard slope using GraphPad Prism 6.0 software (GraphPad, La Jolla, California, USA).

### Immunoblot analysis and antibodies

For immunoblots, cells were lysed as described previously [4]. Whole protein extract from cells was prepared as described [4]. Protein sample concentration was determined by Bradford protein assay, and equal amounts (30  $\mu$ g) of protein were loaded in each well of SDS-polyacrylamide gel. Cell extracts were separated by 10% SDS-PAGE, transferred to polyvinylidene difluoride membrane, and probed as indicated. The following antibodies were used for immunoblot analysis: phosphoglycogen synthase, GAPDH, PARP, and X-linked inhibitor of apoptosis protein (XIAP) (Cell Signaling, Danver, Massachusetts, USA). Bound antibodies were detected as described previously [4].

### Xenograft tumor models

Athymic mice were housed under pathogen-free conditions in accordance with current regulations and standards of the National Institutes of Health. All animal research was approved by Northwestern University Institutional Animal Care and Use Committee. Female athymic nude mice (6–8 weeks old) were inoculated subcutaneously with  $1 \times 10^6$  SK-N-BE(2) or SK-N-DZ neuroblastoma cells mixed with Matrigel (BD Biosciences; Billerica, Massachusetts, USA). Xenograft tumors were staged before initiating the treatment and mice were randomized into four treatment groups: control (DMSO), 9-ING-41, CPT-11, and CPT-11 + 9-ING-41. At the end of the study, subcutaneous xenograft tumors were fixed in 10% formalin and processed to paraffin embedding.

### Immunohistochemical staining and TUNEL

Immunohistochemical staining was performed on paraffin sections of neuroblastoma tissue microarray assay and

xenograft tumors. Paraffin sections were deparaffinized, and antigen retrieval was carried out in citric buffer in microwave for 10 min. The sections were incubated in 1% hydrogen peroxidase for 10 min to quench endogenous tissue peroxidase. Tissue sections were then incubated with the anti-GSK-3 $\beta$  antibody (Cell Signaling) overnight at +4°C. The slides were stained using a standard EnVision+ System-HRP kit (Dako, Carpinteria, California, USA) according to the manufacturer's protocol. Immunohistochemical reactions were developed with diaminobenzidine as the chromogenic peroxidase substrate, and slides were counterstained with hematoxylin. Negative control samples included replacement of the primary antibody with nonimmune IgG1 (Dako). GSK-3 $\beta$  positive expression was defined as positive staining of more than 50% of cancer cells throughout the neuroblastoma tumor section.

TUNEL staining was performed according to manufacturer's protocol (ApopTag Detection Kit; EMD Millipore; Burlington, Massachusetts, USA). The percentage of apoptosis was calculated as the number of TUNEL-positive cells and bodies per 1000 cells counted in three randomly selected microscopic fields in each xenograft tumor sample.

### Statistical analysis

Correlations between GSK-3 $\beta$  immunohistochemical staining of neuroblastoma tissue microarray assay and clinicopathological parameters were analyzed using Fisher's exact test. All other values are presented as mean  $\pm$  SE. Cell viability assay and PDX tumor data were analyzed with one-way analysis of variance. *P* values less than 0.05 were considered significant. Statistical analysis was performed using GraphPad Prism 6.0 software (La Jolla, California, USA).

## Results

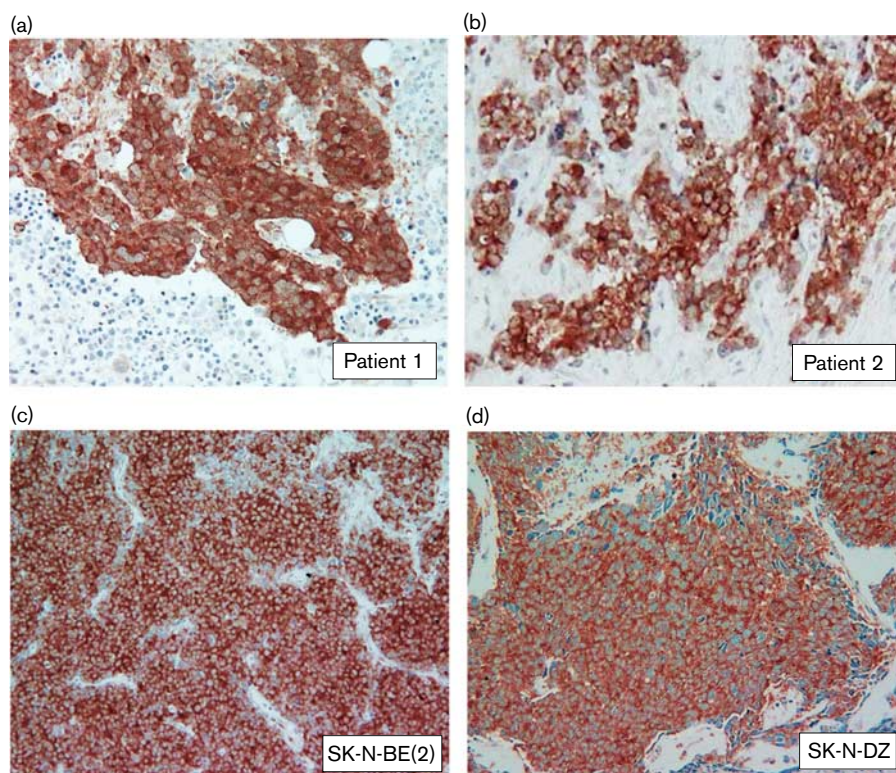
### GSK-3 $\beta$ expression in human neuroblastoma

Using immunohistochemical staining, we found that GSK-3 $\beta$  is highly expressed selectively in cancer cells in 67% of human neuroblastomas (34 of 51 cases) and in subcutaneous xenograft tumors established from SK-N-BE(2) and SK-N-DZ neuroblastoma cell lines (Fig. 1). In human neuroblastoma, GSK-3 $\beta$  expression was not associated with clinical stage, survival or other clinicopathological parameters.

### GSK-3 inhibitor 9-ING-41 decreases neuroblastoma cell viability and potentiates the antitumor effect of CPT-11 *in vitro*

Using neuroblastoma cell lines, we tested the effect of chemically distinct small-molecule inhibitors of GSK-3: AR-A014418, TDZD-8, and 9-ING-41 [18,23,24]. 9-ING-41 has been shown to be more selective for GSK-3 than for 320 other related kinases [20]. Because of the high homology of GSK-3 isoforms, all known competitive

Fig. 1



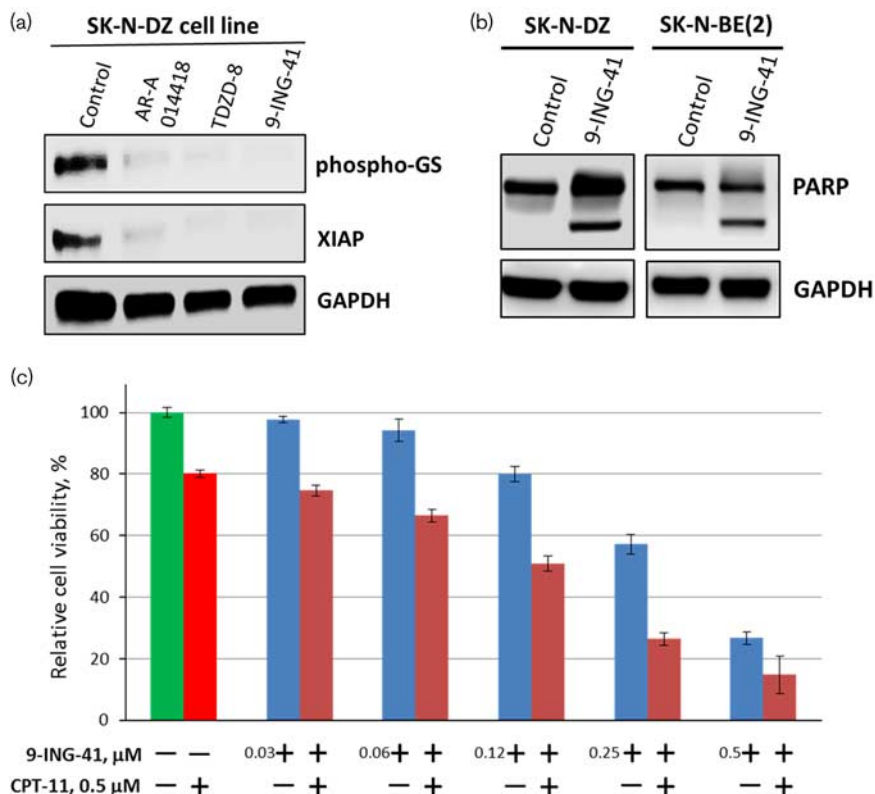
Expression of GSK-3 $\beta$  in human neuroblastoma. (a–d) Representative pictures of GSK-3 $\beta$  expression in human neuroblastoma. GSK-3 $\beta$  is overexpressed in cancer cells in human neuroblastoma tumors obtained from two patients with cancer (a, b) and in xenograft tumors established from SK-N-BE(2) and SK-N-DZ neuroblastoma cell lines (c, d).

inhibitors of GSK-3 $\beta$ , including 9-ING-41, inhibit both GSK-3 $\alpha$  and GSK-3 $\beta$  [18,23,25]. We found that all tested GSK-3 inhibitors suppressed the activity of GSK-3 in neuroblastoma cells as shown by downregulation of phospho-glycogen synthase, a direct downstream target of GSK-3 (Fig. 2a). Moreover, expression of XIAP, an anti-apoptotic protein regulated by NF- $\kappa$ B, was decreased in neuroblastoma cells treated with GSK-3 inhibitors (Fig. 2a). Using a cell viability assay, we found that the GI<sub>50</sub> of GSK-3 inhibitor 9-ING-41 (50–100 nmol/l) for inhibiting the growth of SK-N-DZ and SK-N-BE(2) neuroblastoma cells was 10–60 times lower than the GI<sub>50</sub> of toolkit GSK-3 inhibitors, AR-A014418 and TDZD-8 (data not shown). Our results show that 9-ING-41 (0.1–1  $\mu$ mol/l) inhibits GSK-3, as shown by downregulation of phospho-glycogen synthase expression, leading to a decreased expression of the NF- $\kappa$ B target XIAP and significant apoptosis in neuroblastoma cells as shown by PARP cleavage, an apoptosis marker (Fig. 2a and b).

High-risk or relapsed neuroblastoma is resistant to most chemotherapeutic agents including CPT-11 [26]. A recently published study showed that 9-ING-41 potentiates the antitumor effects of the chemotherapeutic drug CPT-11 in models of breast cancer *in vitro*

and *in vivo* [22]. We tested our hypothesis that inhibition of GSK-3 may overcome resistance to CPT-11 in neuroblastoma cells. Continuous treatment of cancer cell lines with the same concentration of drug for 72 h is not clinically relevant as tumor exposure decreases over time after drug administration owing to drug clearance. Therefore, we used pulses of drug exposure to neuroblastoma cells. Taking into account the plasma half-life of 9-ING-41 (~3 h) and CPT-11 (~8 h), we used the approach of clinically relevant pulsed *in vitro* treatment (5 h) to mimic transient drug exposure *in vivo*. Using this approach, we tested different concentrations of 9-ING-41 (30–500 nmol/l) in combination with 0.5  $\mu$ mol/l of CPT-11 (Fig. 2c). The CPT-11 concentration of 0.5  $\mu$ mol/l is based on its plasma  $C_{max}$  = 0.5  $\mu$ mol/l observed in pediatric patients when CPT-11 is administered intravenously at a dose of 60 mg/m<sup>2</sup> [26]. Neuroblastoma cells were treated with 9-ING-41, CPT-11, or CPT-11 + 9-ING-41 for 5 h (Fig. 2c). After treatment, cells were washed, and all test compounds were replaced with fresh compound-free cell culture media. Neuroblastoma cells were then allowed to continue growing for 72 h, and relative cell growth was measured by a cell viability assay. In SK-N-DZ neuroblastoma cells, we found that monotherapy (5 h) with 0.5  $\mu$ mol/l 9-ING-41 (75% growth inhibition)

Fig. 2



Treatment with GSK-3 inhibitor 9-ING-41 suppresses growth and viability of neuroblastoma cells. (a) SK-N-DZ neuroblastoma cells were treated with 5  $\mu\text{mol/l}$  AR-A014418, 5  $\mu\text{mol/l}$  TDZD-8 and 0.1  $\mu\text{mol/l}$  9-ING-41 for 48 h. Cell lysates were separated by SDS-PAGE, transferred to polyvinylidene difluoride membrane, and probed with antibodies to the indicated proteins. (b) SK-N-DZ and SK-N-BE(2) neuroblastoma cells were treated with 0.1 and 1  $\mu\text{mol/l}$  9-ING-41, respectively. Following 48 h after treatment, cell lysate was prepared and processed as described in (a). (c) SK-N-BE(2) neuroblastoma cells were treated with 9-ING-41, CPT-11, or combination of 9-ING-41 with CPT-11 for 5 h as indicated. After the treatment, drugs were replaced with fresh media and relative cell growth was measured by MTS assay after 72 h. Columns, mean cell viability; bars, SE.

was more effective than treatment with CPT-11 (20% growth inhibition) at the same concentration (Fig. 2c). In these studies, we found that 9-ING-41 potentiates the antitumor effects of 0.5  $\mu\text{mol/l}$  CPT-11 when used at 120 nmol/l ( $P < 0.05$ ) and 250 nmol/l ( $P < 0.05$ ) (Fig. 2c).

**GSK-3 inhibitor 9-ING-41 potentiates the effects of CPT-11 in growth inhibition of neuroblastoma xenograft tumors**

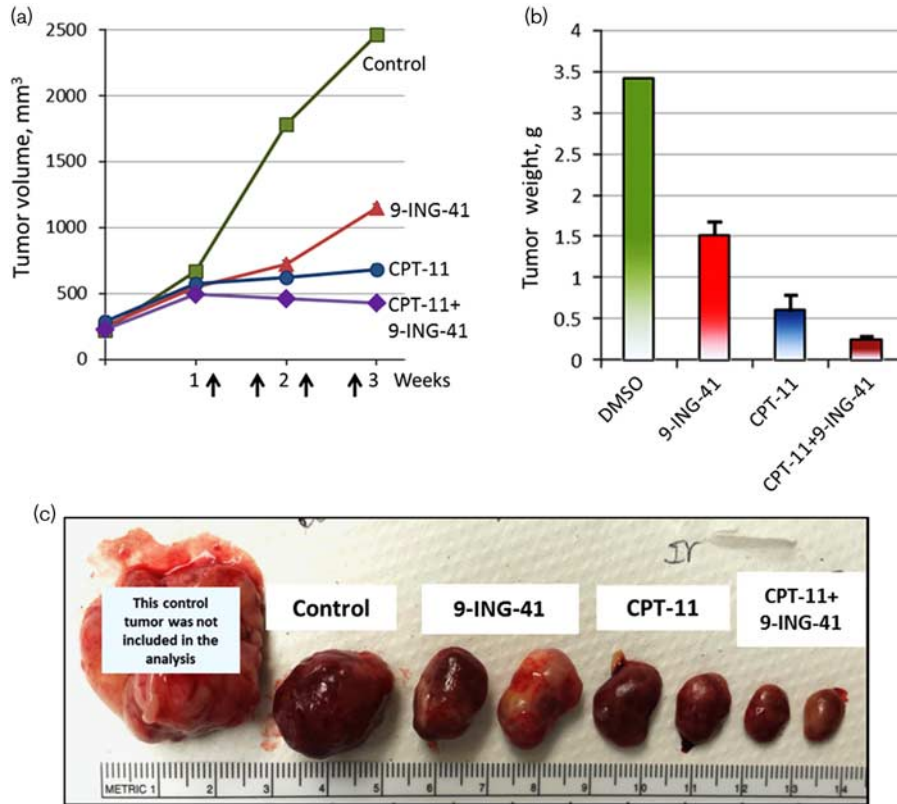
We used subcutaneous SK-N-BE(2) and SK-N-DZ xenograft tumor models to evaluate the antitumor effect of 9-ING-41 alone and in combination with CPT-11 (Figs 3 and 4). Before initiation of the treatment, SK-N-BE(2) and SK-N-DZ xenograft tumors were staged to ~ 500 and 200  $\text{mm}^3$ , respectively. Animals were randomized to four treatment groups: control, 9-ING-41, CPT-11, and CPT-11 + 9-ING-41. Vehicle (DMSO) or drugs were injected intraperitoneally using the schedules indicated (Figs 3 and 4). Our initial screening study showed that the growth of SK-N-BE(2) xenograft tumors was inhibited by 9-ING-41 or CPT-11 monotherapy, and 9-ING-41 + CPT-11 treatment led to SK-N-BE(2) tumor

regression (Fig. 3). Although we found that 9-ING-41 monotherapy did not significantly inhibit SK-N-DZ xenograft tumor growth, combined CPT-11 and 9-ING-41 therapy led to regression of SK-N-DZ tumors (Fig. 4). Analysis of TUNEL staining revealed a significant increase in apoptosis in CPT-11 + 9-ING-41-treated SK-N-DZ xenograft tumors ( $P < 0.05$ ) (Fig. 4c and d).

**Discussion**

Arising from neural crest cells, neuroblastoma is an embryonal tumor accounting for ~ 15% of childhood cancer deaths, with most high-risk neuroblastoma tumors being resistant to chemotherapy, surgery and radiation therapy [1]. There is thus an urgent need for new treatment approaches for this pediatric cancer population. Recently published study identified a specific activation of GSK-3 in neural crest cells as they depart from the neuroepithelium and become migratory mesenchymal cells [27]. GSK-3 activation is controlled by anaplastic lymphoma kinase, which is associated with poor prognosis in patients with neuroblastoma [27]. Examination of nine neuroblastoma cell lines revealed a clear correlation between activation of

Fig. 3



Antitumor effects of 9-ING-41 and CPT-11 treatment in SK-N-BE(2) xenograft model. (a) SK-N-BE(2) neuroblastoma cells were inoculated subcutaneously to eight nude mice (one tumor per mouse). Following 4 weeks after transplantation tumors were size matched and mice were randomized into four treatment groups: control (DMSO;  $n = 2$  mice), GSK-3 inhibitor 9-ING-41 (70 mg/kg;  $n = 2$  mice), CPT-11 (5 mg/kg;  $n = 2$  mice) and CPT-11 + 9-ING-41 ( $n = 2$  mice). Vehicle (DMSO) or drugs were injected as shown by arrows. Points, mean tumor volume; bars, SE. (b) The weight of resected SK-N-BE(2) tumors was measured. Columns, mean tumor weight; bars, SE. (c) Representative pictures of SK-N-BE(2) tumors from each group of animals.

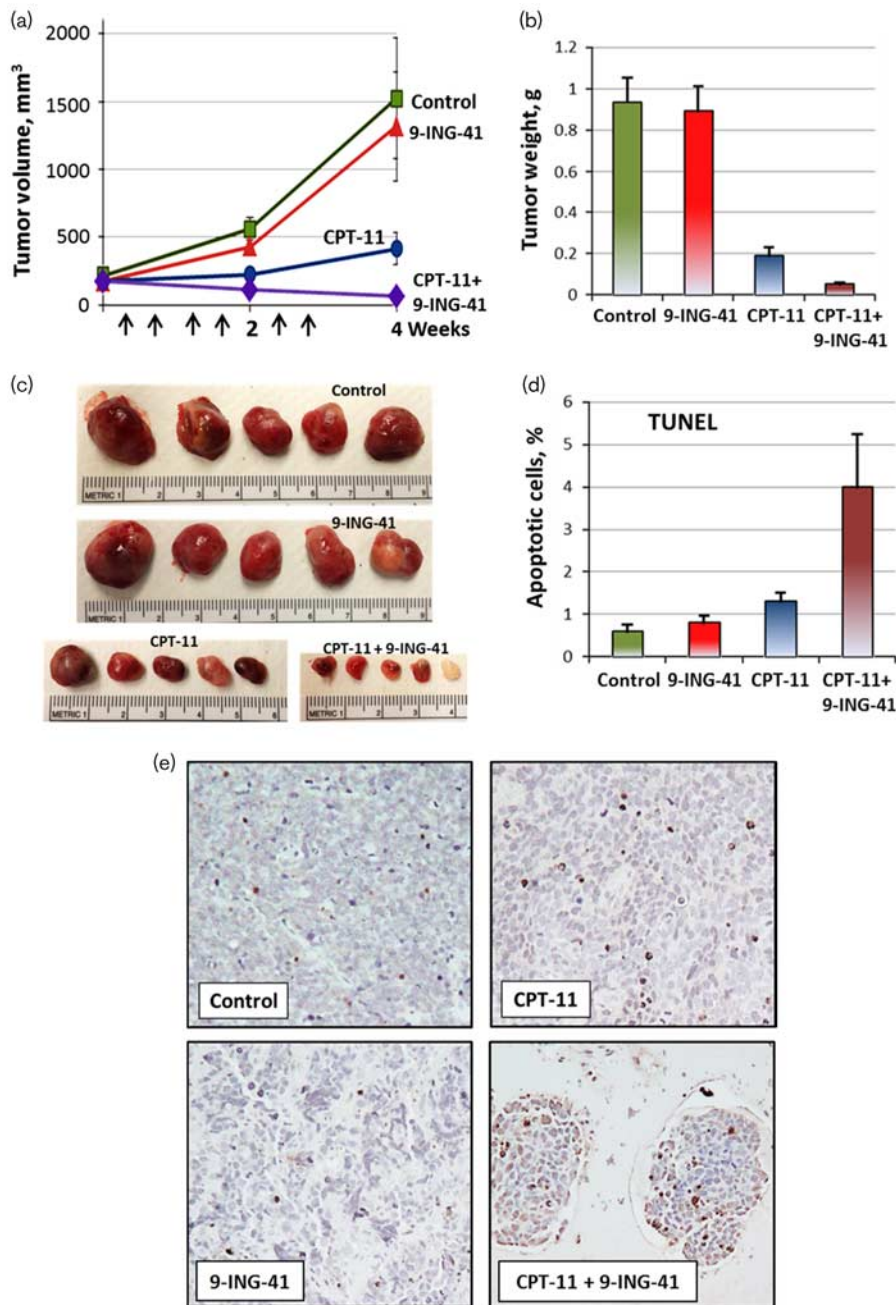
anaplastic lymphoma kinase and GSK-3 [27]. It has been demonstrated that genetic and pharmacological loss of GSK-3 activity leads to cytoskeletal changes in migratory neural crest cells as well as in neuroblastoma cells [27]. Recent studies have established GSK-3 $\beta$ , a positive regulator of NF- $\kappa$ B-mediated survival and chemoresistance of cancer cells [4–10,21,22], as a potential therapeutic target in human neuroblastoma [14–17]. Our data show that GSK-3 $\beta$  expression is highly prevalent in human neuroblastomas supporting a rationale for development of a GSK-3 targeted therapy. Although this study is the first to our knowledge to examine the expression of GSK-3 $\beta$  in human neuroblastomas, a number of other studies have demonstrated GSK-3 $\beta$  protein overexpression in human pancreatic, colon, ovarian, bladder, and breast carcinomas [5,7,9,28,29].

In the present study, we tested a clinical stage GSK-3 small-molecule inhibitor 9-ING-41, which shows profound antitumor activity *in vitro* and *in vivo* [18–22]. We demonstrate that inhibition of GSK-3 by 9-ING-41 decreases the survival of neuroblastoma cells *in vitro*, consistent with previously published studies targeting GSK-3 in

neuroblastoma and other cancer types [4–10,14–22]. Previous studies have demonstrated that the inhibition of GSK-3 decreases cancer cell survival by suppression of the NF- $\kappa$ B-mediated expression of XIAP in different types of cancer [4,6,8,22]. Here, we show that inhibition of GSK-3 by 9-ING-41 led to a decreased expression of XIAP and induction of apoptosis in neuroblastoma cells. These data are consistent with a prior report by Duffy *et al.* [16] who reported a novel GSK-3-mediated regulation of MYC (c-MYC and MYCN) mRNA levels in neuroblastoma. This group also reported that nonclinically applicable GSK-3 inhibitors induced large-scale cell death, by both p53-dependent and independent mechanisms, in neuroblastoma cells, primarily through activating apoptosis [16].

Inhibition of GSK-3 has been shown as a promising approach to overcome chemoresistance of cancer cells and to potentiate chemotherapy [8,21,22,30]. AR-A014418, a toolbox GSK-3 inhibitor, enhanced the anticancer effect of docetaxel and synergistically decreased the viability of renal cancer cells [8]. Similarly, AR-A014418 was shown to sensitize pancreatic cancer

Fig. 4



Treatment with combination of CPT-11 and 9-ING-41 leads to an increased apoptosis and a regression of SK-N-DZ xenograft tumors. SK-N-DZ neuroblastoma cells were inoculated subcutaneously to 20 nude mice (one tumor per mouse). Tumors were size matched, and mice were randomized into four treatment groups: control (DMSO;  $n = 5$  mice), CPT-11 (5 mg/kg,  $n = 5$  mice), 9-ING-41 (70 mg/kg,  $n = 5$  mice) and CPT-11 + 9-ING-41 ( $n = 5$  mice). (a) Vehicle (DMSO) or drugs were injected as shown by arrows. Points, mean tumor volume; bars, SE. (b) The weight of resected tumors was measured. Columns, mean tumor weight; bars, SE. (c) Representative pictures of tumors from each group of animals. (d) The percentage of apoptotic cells was determined by TUNEL staining. Columns, mean apoptotic cells; bars, SE. (e) Representative pictures of TUNEL staining of SK-N-DZ neuroblastoma xenograft tumors treated as indicated.

cells to gemcitabine [30]. Our previous work showed that 9-ING-41 potentiates antitumor effects of selected chemotherapeutic drugs in chemoresistant models of glioblastoma and breast cancer [21,22]. Here, we found that

inhibition of GSK-3 by 9-ING-41 sensitized neuroblastoma cells to CPT-11, a chemotherapeutic drug that has limited clinical activity in human neuroblastoma [26]. As continuous exposure (48–96 h) of neuroblastoma cells

to either 9-ING-41 or a chemotherapeutic drug significantly suppresses cell viability and does not mimic tumor exposure to a drug *in vivo*, we used pulse treatments (5 h) of neuroblastoma cells using concentrations of 9-ING-41 in combination with CPT-11 based on the pharmacokinetics of each drug followed by washout with drug-free cell culture media and then allowed the cells to grow for 72 h. Under these conditions, we found that 9-ING-41 potentiated the antitumor effects of CPT-11 on neuroblastoma cell growth.

These *in vitro* results provided a rationale for further evaluation of 9-ING-41 in neuroblastoma xenograft models. We found that 9-ING-41 monotherapy inhibits the growth of SK-N-BE(2) xenograft tumors. Our findings are supported by another published study showing that treatment with toolkit GSK-3 inhibitor SB415286 suppressed the growth of xenograft tumors established from Neuro-2A neuroblastoma cell line [14]. Our previous *in vivo* studies showed a regression of breast cancer PDX tumors treated with combination of CPT-11 and 9-ING-41 [22]. Here, we found that treatment with the combination of CPT-11 and 9-ING-41 led to regression of established neuroblastoma xenograft tumors. These data are supported by our *in vitro* results showing that 9-ING-41 potentiates the antitumor effect of CPT-11 in neuroblastoma cells at clinically relevant concentrations after short-term exposure. Taken together, our findings provide a rationale for combining 9-ING-41 and CPT-11 as a potential novel therapeutic approach for the treatment of human neuroblastoma.

The Food and Drug Administration has granted 9-ING-41 orphan drug status for the treatment of neuroblastoma, and an investigational new drug application for 9-ING-41 has been recently approved by Food and Drug Administration for the first time in human phase I/II clinical trials. Our results suggest GSK-3 $\beta$  overexpression in neuroblastoma as a potential biomarker for the selection of patients in prospective 9-ING-41 clinical trials. Overall, the results of the current study provide a rationale for the advancement of 9-ING-41 into the clinic for the treatment of neuroblastoma.

## Acknowledgements

This work was supported by generous donations from the Little Heroes Foundation (M.J.H., A.P.M.) and by Cancer Center Support Grant 2 P30 CA060553-19 (A.P.M., A.U.) to the Robert H. Lurie Comprehensive Cancer Center of Northwestern University.

## Conflicts of interest

9-ING-41 has been licensed to Actuate Therapeutics Inc. Andrey V. Ugolkov, Thomas V. O'Halloran, Francis J. Giles, and Andrew Mazar hold an equity interest in Actuate Therapeutics Inc. For the remaining authors, there are no conflicts of interest.

## References

- Whittle SB, Smith V, Doherty E, Zhao S, McCarty S, Zage PE. Overview and recent advances in the treatment of neuroblastoma. *Expert Rev Anticancer Ther* 2017; **17**:369–386.
- Cotran RS, Kumar V, Robbins SL. *Robbins Pathologic Basis of Disease*, 4th ed. Philadelphia, PA: W.B. Saunders Company; 2009.
- Kim WY, Wang X, Wu Y, Doble BW, Patel S, Woodgett JR, et al. GSK-3 is a master regulator of neural progenitor homeostasis. *Nat Neurosci* 2009; **12**:1390–1397.
- Ugolkov A, Fernandez-Zapico M, Savoy D, Urrutia R, Billadeau D. Glycogen synthase kinase-3 $\beta$  participates in nuclear factor kappaB-mediated gene transcription and cell survival in pancreatic cancer cells. *Cancer Res* 2005; **65**:2076–2081.
- Ugolkov A, Fernandez-Zapico M, Bilim V, Smyrk T, Chari S, Billadeau D. Aberrant nuclear accumulation of glycogen synthase kinase-3 $\beta$  in human pancreatic cancer: association with kinase activity and tumor dedifferentiation. *Clin Cancer Res* 2006; **12**:5074–5081.
- Ugolkov A, Bone N, Fernandez-Zapico M, Kay N, Billadeau D. Inhibition of glycogen synthase kinase-3 activity leads to epigenetic silencing of nuclear factor kappaB target genes and induction of apoptosis in chronic lymphocytic leukemia B cells. *Blood* 2007; **110**:735–742.
- Shakoori A, Ugolkov A, Zhang B, Modarressi M, Billadeau D, Mai M, et al. Deregulated GSK3 $\beta$  activity in colorectal cancer: its association with tumor cell survival and proliferation. *Biochem Biophys Res Commun* 2005; **334**:1365–1373.
- Bilim V, Ugolkov A, Yuuki K, Naito S, Kawazoe H, Muto A, et al. Glycogen synthase kinase-3: a new therapeutic target in renal cell carcinoma. *Br J Cancer* 2009; **101**:2005–2014.
- Naito S, Bilim V, Yuuki K, Ugolkov A, Motoyama T, Nagaoka A, et al. Glycogen synthase kinase-3 $\beta$ : a prognostic marker and a potential therapeutic target in human bladder cancer. *Clin Cancer Res* 2010; **16**:5124–5132.
- Walz A, Ugolkov A, Chandra S, Kozikowski A, Carneiro BA, O'Halloran TV, et al. Molecular pathways: revisiting Glycogen Synthase Kinase-3 $\beta$  as a target for the treatment of cancer. *Clin Cancer Res* 2017; **23**:1891–1897.
- Bian X, Opiari AW Jr, Ratanaproeksa AB, Boitano AE, Lucas PC, Castle VP. Constitutively active NF $\kappa$ B is required for the survival of S-type neuroblastoma. *J Biol Chem* 2002; **277**:42144–42150.
- Karacay B, Sanlioglu S, Griffith TS, Sandler A, Bonthius DJ. Inhibition of the NF- $\kappa$ B pathway enhances TRAIL-mediated apoptosis in neuroblastoma cells. *Cancer Gene Ther* 2004; **11**:681–690.
- Ammann JU, Haag C, Kasperczyk H, Debatin KM, Fulda S. Sensitization of neuroblastoma cells for TRAIL-induced apoptosis by NF- $\kappa$ B inhibition. *Int J Cancer* 2009; **124**:1301–1311.
- Dickey A, Schleicher S, Leahy K, Hu R, Hallahan D, Thotala D. GSK-3 $\beta$  inhibition promotes cell death, apoptosis, and *in vivo* tumor growth delay in neuroblastoma Neuro-2A cell line. *J Neurooncol* 2011; **104**:145–153.
- Carter Y, Kunnimalaiyaan S, Chen H, Gambin T, Kunnimalaiyaan M. Specific glycogen synthase kinase-3 inhibition reduces neuroendocrine markers and suppresses neuroblastoma cell growth. *Cancer Biol Ther* 2014; **15**:510–515.
- Duffy DJ, Krstic A, Schwarzl T, Higgins DG, Kolch W. GSK3 inhibitors regulate *MYCN* mRNA levels and reduce neuroblastoma cell viability through multiple mechanisms, including p53 and Wnt signaling. *Mol Cancer Ther* 2014; **13**:454–467.
- Mathuram TL, Ravikumar V, Reece LM, Karthik S, Sasikumar CS, Cherian KM. Tideglusib induces apoptosis in human neuroblastoma IMR32 cells, provoking sub-G0/G1 accumulation and ROS generation. *Environ Toxicol Pharmacol* 2016; **46**:194–205.
- Gaisina I, Gallier F, Ugolkov A, Kim K, Kurome T, Guo S, et al. From a natural product lead to the identification of potent and selective benzofuran-3-yl-(indol-3-yl)maleimides as glycogen synthase kinase 3 $\beta$  inhibitors that suppress proliferation and survival of pancreatic cancer cells. *J Med Chem* 2009; **52**:1853–1863.
- Hilliard T, Gaisina I, Muehlbauer A, Gaisina A, Gallier F, Burdette J. Glycogen synthase kinase 3 $\beta$  inhibitors induce apoptosis in ovarian cancer cells and inhibit *in vivo* tumor growth. *Anticancer Drugs* 2011; **22**:978–985.
- Pal K, Cao Y, Gaisina IN, Bhattacharya S, Dutta SK, Wang E, et al. Inhibition of GSK-3 induces differentiation and impaired glucose metabolism in renal cancer. *Mol Cancer Ther* 2014; **13**:285–296.
- Ugolkov A, Qiang W, Bondarenko G, Procissi D, Gaisina I, James CD, et al. Combination treatment with the GSK-3 inhibitor 9-ING-41 and CCNU cures orthotopic chemoresistant glioblastoma in patient-derived xenograft models. *Transl Oncol* 2017; **10**:669–678.
- Ugolkov A, Gaisina I, Zhang JS, Billadeau DD, White K, Kozikowski A, et al. GSK-3 inhibition overcomes chemoresistance in human breast cancer. *Cancer Lett* 2016; **380**:384–392.

- 23 Bhat R, Xue Y, Berg S, Hellberg S, Ormö M, Nilsson Y, *et al.* Structural insights and biological effects of glycogen synthase kinase 3-specific inhibitor AR-A014418. *J Biol Chem* 2003; **278**:45937–45945.
- 24 Martinez A, Alonso M, Castro A, Perez C, Moreno FJ. First non-ATP competitive glycogen synthase kinase 3 beta (GSK-3beta) inhibitors: thiazolidinones (TDZD) as potential drugs for the treatment of Alzheimer's disease. *J Med Chem* 2002; **45**:1292–1299.
- 25 Coghlan MP, Culbert AA, Cross DA, Corcoran SL, Yates JW, Pearce NJ, *et al.* Selective small molecule inhibitors of glycogen synthase kinase-3 modulate glycogen metabolism and gene transcription. *Chem Biol* 2000; **7**:793–803.
- 26 Furman WL, Crews KR, Billups C, Wu J, Gajjar AJ, Daw NC, *et al.* Cefixime allows greater dose escalation of oral irinotecan: a phase I study in pediatric patients with refractory solid tumors. *J Clin Oncol* 2006; **24**:563–570.
- 27 Gonzalez Malagon SG, Lopez Munoz AM, Doro D, Bolger TG, Poon E, Tucker ER, *et al.* Glycogen synthase kinase controls migration of the neural crest lineage in mouse and xenopus. *Nat Commun* 2018; **9**:1126.
- 28 Rask K, Nilsson A, Brannstrom M, Carlsson P, Hellberg P, Janson PO, *et al.* Wnt signalling pathway in ovarian epithelial tumours: increased expression of beta-catenin and GSK3beta. *Br J Cancer* 2003; **89**:1298–1304.
- 29 Quintayo MA, Munro AF, Thomas J, Kunkler IH, Jack W, Kerr GR, *et al.* GSK3 $\beta$  and cyclin D1 expression predicts outcome in early breast cancer patients. *Breast Cancer Res Treat*, **136**2012. 161–168.
- 30 Shimasaki T, Ishigaki Y, Nakamura Y, Takata T, Nakaya N, Nakajima H, *et al.* Glycogen synthase kinase-3 $\beta$  inhibition sensitizes pancreatic cancer cells to gemcitabine. *J Gastroenterol* 2012; **47**:321–333.